A Disease State Mutation Unfolds the Parkin Ubiquitin-like Domain†

Susan S. Safadi and Gary S. Shaw*

Department of Biochemistry, The University of Western Ontario, London, Ontario, Canada, N6A 5C1

Received August 21, 2007; Revised Manuscript Received October 9, 2007

ABSTRACT: E3 ubiquitin ligases are essential enzymes in the ubiquitination pathway responsible for the recognition of specific E2 conjugating enzymes and for transferring ubiquitin to a substrate targeted for degradation. In autosomal recessive juvenile Parkinson's disease, an early onset form of Parkinson's disease, point mutations in the E3 ligase parkin are one of the most commonly observed traits. Parkin is a multidomain E3 ligase that contains an N-terminal ubiquitin-like domain that interacts with, and effects the ubiquitination of, substrates such as cyclin E, p38 and synphilin. In this work we have examined the folding and structure of the parkin ubiquitin-like domain (Ubld) and of the protein with two causative disease mutations (K48A and R42P). Parallel experiments with the protein ubiquitin were done in order to determine if the same mutations were detrimental to the ubiquitin structure and stability. Despite similar folds between the parkin Ubld and ubiquitin, urea unfolding experiments show that the parkin Ubld is surprisingly ~10.6 kJ/mol less stable than ubiquitin. The K48A mutation had little effect on the stability of the parkin Ubld or ubiquitin indicating that this mutation contributes to defective protein−protein interactions. In contrast, the single point mutation R42P in parkin's Ubld caused poor expression and degradation of the protein. To avoid these problems, a GB1-Ubld fusion protein was characterized by NMR spectroscopy to show that the R42P mutation causes the complete unfolding of the parkin Ubld. This observation provides a rationale for the more rapid degradation of parkin carrying the R42P mutation *in vivo*, and its inability to interact with some substrate proteins. Our work provides the first structural and folding insight into the effects of causative mutations within the ubiquitin-like domain in autosomal recessive juvenile Parkinson's disease.

Autosomal recessive juvenile Parkinsonism (ARJP[1]) is an early onset familial form of Parkinson's disease (PD) that is clinically indistinguishable from the more prevalent idiopathic form of PD. Mutations in ARJP patients have been identified in several genes, although the most commonly mutated gene encodes an E3 ubiquitin-protein ligase termed parkin (*1*−*3*). Mutations in parkin account for approximately 50% of all ARJP cases. E3 ligases such as parkin are essential enzymes in the ubiquitination pathway. This pathway culminates with the covalent attachment of the small, 76 amino acid protein ubiquitin to one or more of the lysine side chains of a cellular protein. The modification is an essential biochemical process that signals or regulates protein degradation via the 26S proteasome and non-proteolytic processes such as cell cycle and cell division, activation and silencing of transcription, endocytosis and DNA repair (*4*−*6*). Three enzymes in this pathway (E1, E2 and E3) transfer the ubiquitin protein to its final destination on the targeted protein. The E3 enzymes play an important role in mediating the transfer of ubiquitin onto the target protein through their interaction with both the E2 enzyme and substrate and provide the specificity for target protein recognition.

Parkin is a multidomain E3 ligase consisting of 465 amino acids and 5 distinct domains including an N-terminal ubiquitin-like domain (Ubld) followed by a unique parkin specific domain (UPD) and two C-terminal RING domains separated by an in-between RING (IBR) domain. The C-terminus of parkin has been shown to function in conjunction with the E2 ubiquitin conjugating enzymes UbcH7 (*3*) and UbcH8 (*7*) leading to ubiquitination of substrates such as cyclin E (*8*), p38 (*9*) and synphilin (*10*). The N-terminal domains, Ubld and UPD, while not directly involved in E2 interactions, have both been shown to be essential for the ligase activity of parkin since deletion or mutation of these domains results in impaired E3 ligase activity (*3*, *11*−*13*). The Ubld from parkin has been shown to be involved in many specific interactions. Two of these interactions involve binding to the ubiquitin interacting motifs (UIMs) found in the proteasomal subunit S5a and the endocytic protein Eps15 (*14*, *15*). Data has also shown that the Ubld participates in interactions with the F-box/WD repeat protein hSel-10 thus implicating parkin's involvement in an SCF-like ubiquitin ligase complex (*8*). The Ubld shares 32% sequence identity with ubiquitin as well as a similar three-dimensional fold. Integral Ublds are a common feature in many multidomain proteins whose other domains are involved in diverse processes (*16*, *17*). Some representative members include hPLIC-2 (DSK2 in yeast) involved in spindle body duplication, Bag1 a chaperone protein, and the E3 ligases, parkin

† This research was supported by research and maintenance grants from the Canadian Institutes of Health Research (G.S.S.) and awards from the Canada Research Chairs (G.S.S.) and Canadian Graduate Scholarship (S.S.S.) programs.

* Author to whom correspondence should be addressed. Phone: 519-661-4021. Fax: 519-661-3175. E-mail: gshaw1@uwo.ca. Web: www.biochem.uwo.ca/fac/shaw.

[1] Abbreviations: ARJP, autosomal recessive juvenile Parkinson's disease; Ubld, ubiquitin-like domain; UPD, unique parkin specific domain; GB1, B1 immunoglobulin binding domain from protein G; GB1-Ubld, fusion protein of GB1 linked to N-terminal of Ubld; $Ubld^{R42P}$, R42P mutant Ubld protein; $Ubld^{K48A}$, K48A mutant Ubld protein.

10.1021/bi7016969 CCC: $37.00
Published on Web 11/16/2007

and HOIL-1 involved in ubiquitination (*1*, *18*−*20*). Although this domain is structurally similar to ubiquitin, it does not have the ability to be conjugated to other proteins as observed for ubiquitin.

Mutations associated with ARJP are found throughout the parkin protein. The effects of the disease state mutations localized to the Ubld have been shown to decrease the stability of the full-length parkin protein although to date conflicting evidence has been presented for the effects of the mutations on E3 ligase activity (*11*, *21*, *22*). In all of these studies it has not been possible to distinguish whether the observations arise from mutations causing structural alterations in parkin and/or are a result of disrupted protein interactions with E2 enzymes or potential substrates. One reason for this uncertainty has been the inability to purify parkin, its constitutive domains and especially proteins containing disease-causing mutations. To date, only the parkin Ubld (*14*) and IBR (*23*) domains have been purified and had their three-dimensional structures determined. In addition, while some mutated forms of the parkin IBR domain have been isolated and characterized (*23*), similar approaches have failed for the Ubld mutant containing proteins. In this work we have examined the structure and stability of wild-type Ubld and the protein carrying the R42P ($Ubld^{R42P}$) and K48A ($Ubld^{K48A}$) disease-state mutations (*24*, *25*). Parallel experiments have been carried out with ubiquitin since ubiquitin carries a similar fold as the Ubld. Despite this structural similarity the parkin Ubld is surprisingly much less stable than ubiquitin. Further, our results show that the R42P mutation causes the global unfolding of the parkin Ubld and significantly decreases the stability of ubiquitin. To show this conclusively for parkin, a fusion protein for the parkin $Ubld^{R42P}$ in tandem with the immunoglobulin binding protein domain for protein G (GB1) was expressed, purified and characterized by NMR spectroscopy. In the absence of the GB1 domain the $Ubld^{R42P}$ protein could not be isolated. This work provides evidence that this ARJP disease state mutation results in the drastic alteration of the Ubld structure leading to dysfunction of the protein in the ubiquitination pathway.

EXPERIMENTAL PROCEDURES

Cloning. The DNA fragment encoding the Ubld (residues 1−77) of human parkin was cloned into the *Nde*I and *Bam*HI sites of the pET44a vector (Novagen). For expression with an in-frame N-terminal GB1 fusion the DNA fragment encoding the Ubld (1−77) was cloned into the *Nhe*I and *Xho*I sites of the GEV1 vector (*26*), a generous gift from Dr. M. Clore (NIDDK, Bethesda, MD). Ubiquitin from *Saccharomyces cerevisiae* was expressed from a pET3a vector as previously described (*27*). The mutants R42P, K48A in both Ubld and ubiquitin proteins were created using the QuikChange Site-Directed Mutagenesis Kit (Stratagene, La Jolla, CA).

Protein Expression and Purification. All Ubld constructs, GB1, GB1 fusion proteins and mutants of ubiquitin were overexpressed in the BL21(DE3) Codon Plus *Escherichia coli* strain. The bacteria were grown at 37 °C overnight in LB media (10 mL) containing the antibiotic carbenecillin (50 μg/mL) and chloramphenicol (34 mg/mL). The culture was diluted 1:100 in LB media (10 mL in 1 L) containing the same antibiotics. Expression was induced at an OD_{600} of 0.6−0.7 by the addition of 1 mM IPTG and allowed to grow overnight at 15 °C with constant shaking. Ubiquitin was expressed in the BL21(DE3)pLysS *Escherichia coli* strain. The bacteria were grown at 37 °C overnight in LB media (10 mL) containing the antibiotic carbenecillin (50 μg/mL) and chloramphenicol (34 mg/mL). The culture was diluted 1:100 in LB media containing the same antibiotic and induced when an OD_{600} of 0.4 was reached by the addition of 0.4 mM IPTG. The cells were allowed to grow for 4 h at 37 °C with constant shaking. For the production of ^{15}N-labeled proteins, cells were grown in M9 minimal media containing 1.0 g/L $^{15}NH_4Cl$. Ubiquitin and its mutant proteins were purified using a HiTrap Q XL column, followed by size exclusion chromatography at pH 8 as previously described (*27*). All Ubld constructs were purified using similar chromatographic methods except that the pH was increased to 9.0 and 1 mM DTT was added. The isolated GB1 domain was purified on an IgG sepharose column (Amersham) and eluted with 0.5 M sodium acetate pH 3.5 as previously described (*26*). The integrity of all proteins was confirmed by electrospray ionization mass spectrometry (Biological Mass Spectrometry Laboratory, University of Western Ontario).

Protein Unfolding Experiments. Stock denaturant solutions were made of 10 mM KH_2PO_4, 1 mM EDTA, 1 mM DTT and 9 M urea at pH 7.0. The urea stock solution concentration was determined by refractometry (*28*). Protein samples for unfolding experiments were prepared by combining aliquots from a series of protein stock solutions with appropriate dilutions of urea and buffer to provide the desired urea concentration. Samples were equilibrated overnight at 5 °C. Protein stock concentrations were determined by their extinction coefficient in guanidine hydrochloride (*29*).

Unfolding experiments were conducted by urea and thermal denaturation and monitored by circular dichroism spectropolarimetry using a Jasco J-810 instrument (Biomolecular Interactions and Conformations Facility, University of Western Ontario). Protein concentrations ranged from 20 to 80 μM. For each urea concentration, spectra for 10 scans (250−190) were recorded and averaged at 5 °C. For the thermal unfolding experiments the temperature was increased from 5 °C to 100 °C at both 30 °C and 50 °C per hour. A 1 mm path length cell was used and the buffer background was subtracted. All unfolding experiments were conducted in duplicate.

Data Analysis. The chemical unfolding data recorded by circular dichroism spectropolarimetry were analyzed using the program GraphPad Prism version 4.0 (GraphPad Software) on an Apple iMac G3 computer. The unfolding transitions were fit according to a two-state unfolding curve using eqs 1−3 (*30*) where F is the population of the folded protein, U is the population of the unfolded protein and K_u is the equilibrium constant for unfolding.

$$\mathrm{F} \rightleftarrows \mathrm{U} \tag{1}$$

$$K_u = [\mathrm{U}]/[\mathrm{F}] \tag{2}$$

$$K_u = \exp((\Delta G_u^{H_2O} + m[\mathrm{D}])/(-RT)) \tag{3}$$

$$Y_{obs} = (Y_f + Y_u K_u)/(1 + K_u) \tag{4}$$

The free energy difference ($\Delta G_u^{H_2O}$) between the folded and unfolded forms of the protein and the slope of the unfolding transition (m) were determined by a nonlinear global analysis of multiple data sets for the dependence of the observed CD signal (Y_{obs}) as a function of urea concentration ([D]) according to eq 4 (*31*). The baselines prior to (Y_f) and following (Y_u) the unfolding transition were also fit to the linear relationships shown in eqs 5 and 6 where m_f and m_u are the slopes of the pre- and post-unfolding transition and Y_f^0 and Y_u^0 are the intercepts for the folded and unfolded states respectively.

$$Y_f = Y_f^0 + m_f[D] \quad (5)$$

$$Y_u = Y_u^0 + m_u[D] \quad (6)$$

CD data were fit by measuring the ellipticity at both 222 and 230 nm as a function of urea concentration at 278 K. Initial fits of the data showed that the pre- and post-transition slopes (m_f, m_u) were very close to zero. As a result these parameters were set to 0 during final fitting so as to prevent unrealistic fits.

In addition to $\Delta G_u^{H_2O}$ the midpoint of each unfolding curve where 50% of the protein was unfolded ($D_{50\%}$) was determined by incorporating $\Delta G_u^{H_2O} = m(D_{50\%})$ into eq 4 (*32*). The value of $D_{50\%}$ has been shown to be very reproducible (*33*) and provides a more accurate representation of the differences in stability between the wild-type and mutant proteins ($\Delta\Delta G_u^{D_{50\%}}$) according to

$$\Delta\Delta G_u^{D_{50\%}} = \bar{m}\Delta D_{50\%} \quad (7)$$

where $\Delta D_{50\%}$ is the difference between $D_{50\%}$ for the wild-type and mutant proteins respectively and $\bar{m}$ is the average slope for the two proteins (*32*).

NMR Spectroscopy. NMR experiments were performed on a 600 MHz Varian Inova spectrometer equipped with a ^{13}C-enhanced triple resonance cold probe. Sensitivity enhanced $^1H-^{15}N$ HSQC spectra (*34*) were recorded at 25 °C on ^{15}N-labeled Ubld, GB1, GB1-Ubld and GB1-Ubld^{R42P}, samples in 10 mM KH_2PO_4, 1 mM EDTA, 5 mM DTT, 30 μM DSS, 10% D_2O at pH 7.0. All spectra were processed with NMRPipe (*35*) software using a cosine-squared function in ^1H and ^{15}N to minimize artefacts in the spectra and analyzed by using NMRView (*36*).

Size Exclusion Chromatography. All samples were prepared in 10 mM KH_2PO_4, 1 mM EDTA, 1 mM DTT at pH 7.0. For each experiment, (500 μL) samples were injected onto a Superdex 75 column (Amersham) equilibrated in the same buffer and run at room temperature at a flow rate of 0.5 mL/minute. The absorbance at 280 nm was used to determine protein elution volumes.

RESULTS

The three-dimensional structure of the parkin Ubld has been determined by NMR spectroscopy at 30 °C (*14*). The structure comprises a β-grasp fold (Figure 1) containing a five-strand β-sheet (β1, H11−V15; β2, I2−F7; β3, R42−F45; β4, K48−L50; and β5, Q64−V70) and two α-helices (α1, I23−R33; α2, Q57−D60), characteristic of other ubiquitin-like domains such as hPLIC-2 and hHR23a

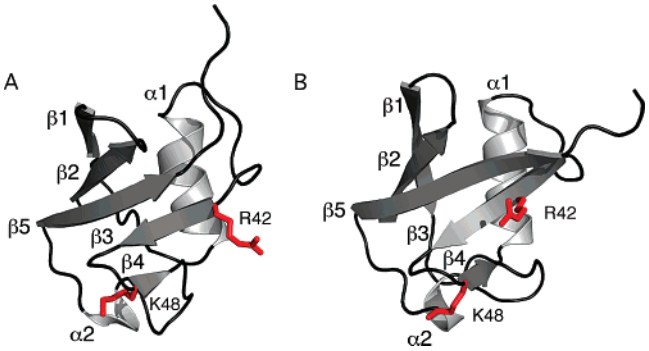

FIGURE 1: Ribbon drawings of the (A) parkin Ubld and (B) ubiquitin. Each structure shows the positions of the β-sheets (β1-β5) and α-helices. The positions of the two mutations studied (R42P and K48A) are indicated with sticks to designate the side chain positions in the proteins. This figure was produced using the program Pymol (*47*) and the PDB files for parkin Ubld (1IYF) (*14*) and ubiquitin (1UBQ) (*48*).

(*37*, *38*). Several mutations found in patients with autosomal recessive juvenile Parkinson's disease are found in the parkin Ubld. Two such mutations, R42P and K48A, are found at the N-termini of sheets β3 and β4 respectively. The structure of ubiquitin (Figure 1) is very similar to the parkin Ubld comprising five β-sheets (β1, G10−V17; β2, M1−T7; β3, Q40−F45; β4, K48−L50; and β5, E64−R72), one regular α-helix (α1, I23−E34) and an α-helix-like turn (L56−Y59). These structural similarities result in a backbone rmsd of 1.38 Å between the two proteins when considering the common sections of the β-sheet regions. Due to this strong similarity in the protein folds in parkin's Ubld and ubiquitin, the ARJP mutations R42P and K48A were constructed in both proteins to determine the differences these mutations make in their structures and stabilities.

Parkin Ubld Has a Lower Stability Compared to Ubiquitin. The folded states of the parkin Ubld and ubiquitin were initially characterized by CD spectropolarimetry. At 5 °C the CD spectrum of ubiquitin had well-defined minima at 208 and 225 nm (Figure 2A), consistent with its three-dimensional structure (Figure 1B) that showed approximately 21% α-helix and 43% β-sheet secondary structure content. The minima present in the Ubld spectrum were shifted from the ubiquitin spectrum and located at 204 and 222 nm. The location of the minimum at 204 nm is characteristic of a protein with greater random coil structure. The differences in the two CD spectra also reflect the longer β-sheets (β1, β3 and β5) observed in ubiquitin compared to the parkin Ubld resulting in decreased β-sheet secondary structure content in the parkin Ubld (31%) compared to ubiquitin (43%).

Initial temperature studies monitored by CD and NMR spectroscopy were used to determine the optimal temperature for further experiments since no information on the stability of the parkin Ubld was available. For the parkin Ubld a decreased intensity for the 222 nm band was observed at temperatures above 5 °C (Figure 2B). Changes in the $^1H-^{15}N$ HSQC NMR spectrum were also noted as the temperature was lowered to 5 °C. The melting curves for native parkin Ubld and ubiquitin indicated that the melting temperature (T_m) for the parkin Ubld occurred around 65 °C which was significantly lower than ubiquitin where the T_m occurred near 85 °C (Figure 2B). As a result of the temperature sensitive spectral changes noted for the parkin

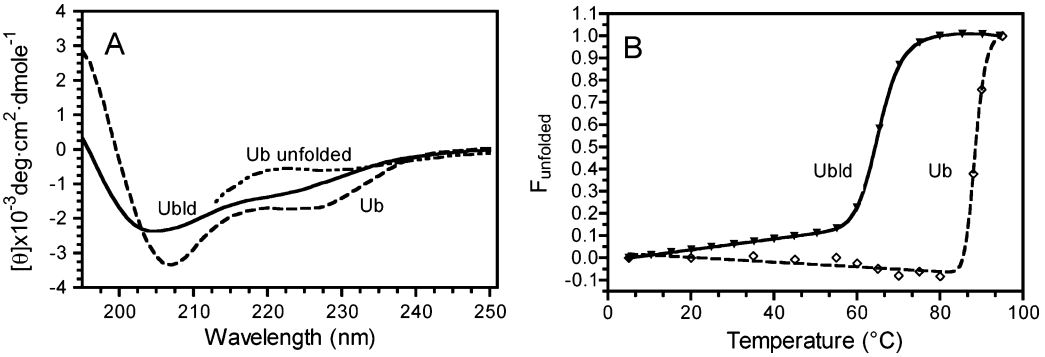

FIGURE 2: CD spectra of parkin Ubld and ubiquitin. (A) The spectra show the CD data for Ubld in the folded (—), ubiquitin in the folded state (– – –), and unfolded states (– ·· –). All samples were composed of 80 μM protein in 10 mM KH_2PO_4, 1 mM EDTA, pH 7 at 5 °C and the addition of 1 mM DTT for the parkin Ubld. The unfolded spectrum of ubiquitin was collected in the presence of 8.5 M urea. (B) Thermal denaturation of the Ubld (—) and ubiquitin (– – –) monitored by CD at 222 nm. Samples were prepared under identical conditions as described above.

Ubld that might arise from unfolding or structural changes in the domain we elected to do all further studies at 5 °C.

Urea denaturation of the parkin Ubld, ubiquitin and their mutants in 8 M urea revealed that the unfolded forms of these proteins had characteristic CD spectra marked by near zero ellipticity at 222 nm and a broad featureless minimum near 230 nm (Figure 2A). Using these two wavelengths the unfolding of each protein was examined as a function of urea denaturant (Figure 3A). In all cases the observed unfolding transitions were marked by smooth sigmoidal curves indicative of a two-state unfolding process (eq 1), although more complicated unfolding pathways have been proposed for ubiquitin (*39*). The data show that there is a clear difference between ubiquitin and the parkin Ubld despite the similarities in their structures. Ubiquitin has a transition midpoint ($D_{50\%}$) near 6.7 M urea while that of the Ubld is much lower (4.85 M). However the slopes of the unfolding curves for both proteins are comparable (Table 1) indicating that the cooperativities for unfolding are probably similar. Fitting of the data resulted in a free energy of unfolding ($\Delta G_u^{H_2O}$) for ubiquitin (24.5 kJ/mol) that was approximately 10.6 kJ/mol higher than the parkin Ubld (13.9 kJ/mol). This increased stability of ubiquitin compared to the parkin Ubld is in agreement with our thermal unfolding observations.

Disease-State Mutations Dramatically Affect Ubiquitin and Ubld Stabilities. The two selected ARJP disease-state mutations R42P and K48A were created in the parkin Ubld as well as in ubiquitin for comparative studies. In both proteins the K48A mutation was found to have little effect on stability compared to the wild-type sequences based on the similarities of the $D_{50\%}$ values (Table 1). In addition the slope of the unfolding transitions for Ubld^{K48A} and Ub^{K48A} were nearly identical to those for the parent proteins. This resulted in $\Delta\Delta G_u^{D_{50\%}}$ values of only 2.3 and 1.0 kJ/mol between the K48A mutants and the Ubld and Ub wild-type proteins respectively (Table 1).

In contrast to the Ubld^{K48A} and Ub^{K48A} proteins, the R42P mutations in the parkin Ubld and ubiquitin had dramatic effects on their expression and the cellular stabilities of these proteins. For example, the Ubld^{R42P} was susceptible to degradation at its N-terminus during expression and purification. Analysis of the partly purified Ubld^{R42P} protein by mass spectrometry indicated a loss of 1609 Da consistent with proteolysis of the first 13 amino acids of the protein. Due to

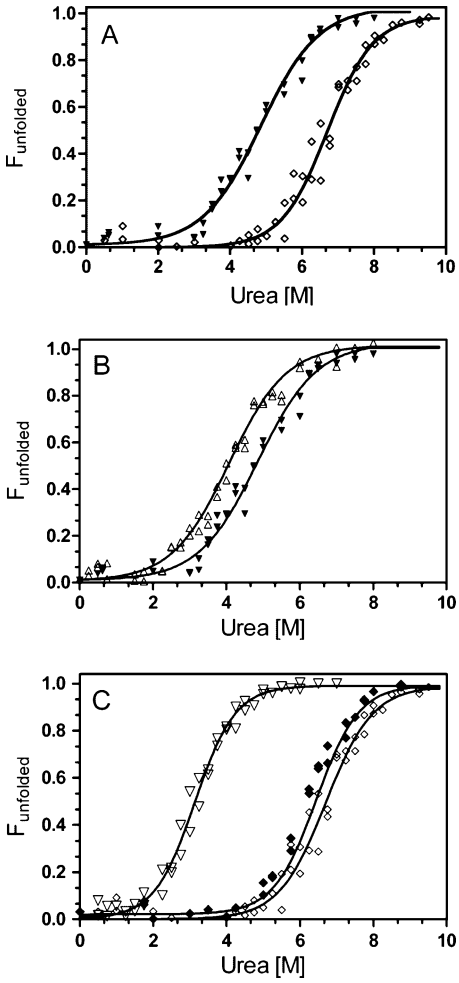

FIGURE 3: Unfolding curves for parkin Ubld, ubiquitin and their mutants. (A) Comparison of the denaturation curves for the Ubld (▼) and ubiquitin (◇). (B) Denaturation curve for Ubld (▼) and K48A (Δ) mutant. (C) Denaturation curve for ubiquitin (◇), K48A (◆) and R42P (▽) mutants. In all cases, data was collected for samples containing various amounts of urea that had been equilibrated with the protein overnight. CD spectra were collected and the ellipticity, measured at 222 and 230 nm, was converted to fraction unfolded. The curves shown were globally fit to multiple data sets according to the equations described in the Experimental Procedures section. The pre- and post-transition slopes (m_f, m_u) were set to 0 during final fitting so as to prevent unrealistic fits. All samples were composed of 20−80 μM protein in 10 mM KH_2PO_4, 1 mM EDTA, pH 7 at 5 °C and the addition of 1 mM DTT for the parkin Ubld.

Table 1: Free Energies of Unfolding Determined by Urea Denaturation

protein	$D_{50\%}$[a] (M)	m[b] (kJ·mol^{-1}·M^{-1})	$\Delta G_u^{H_2O}$ (kJ·mol^{-1})	$\Delta\Delta G_u^{D_{50\%}}$ [c] (kJ·mol^{-1})
Ub	6.71 ± 0.04	−3.7 ± 0.2	24.5 ± 1.5	
K48A	6.44 ± 0.03	−4.0 ± 0.2	25.6 ± 1.1	−1.0 ± 0.2
R42P	3.13 ± 0.03	−4.2 ± 0.2	13.1 ± 0.6	−14.1 ± 0.5
Ubld	4.85 ± 0.06	−2.9 ± 0.2	13.9 ± 0.9	
K48A	4.08 ± 0.05	−3.0 ± 0.2	12.1 ± 0.7	−2.4 ± 0.3

[a] The $D_{50\%}$ is the midpoint of unfolding. [b] The slope m and unfolding free energy were measured using eqs 1−6 as described in the Experimental Procedures. In all cases the pre- and post-transition slopes (m_u, m_f) were set to 0. [c] $\Delta\Delta G_u^{D_{50\%}}$ was calculated according to the equation $\Delta\Delta G_u^{D_{50\%}} = \bar{m}\Delta D_{50\%}$ relative to the respective wild-type protein.

the susceptibility to degradation of the Ubld^{R42P} the unfolding of this protein could not be analyzed by CD spectropolarimetry. However, this vulnerability of Ubld^{R42P} to degradation indicated a marked decrease in stability for this protein in solution. In contrast, the Ub^{R42P} protein did not suffer from proteolysis in solution. This was confirmed by unfolding studies that showed a remarkable 3.6 M shift in its denaturation midpoint (Figure 3C, Table 1). This resulted in a $\Delta\Delta G_u^{D_{50\%}}$ about 14.1 kJ/mol lower for Ub^{R42P} compared to the wild-type protein. Interestingly, the Ub^{R42P} protein had a $\Delta G_u^{H_2O}$ that was similar to that obtained for the wild-type parkin Ubld. While not observed for Ub^{R42P} the increased degradation during expression and purification of the parkin Ubld^{R42P} indicates that at least a comparable 40% decrease in stability might be expected for the Ubld rendering it more susceptible to proteolysis.

The Disease State Mutation R42P in Parkin Unfolds Its Ubiquitin-like Domain. The proteolytic susceptibility of the Ubld^{R42P} indicated that significant alterations to the tertiary structure of the protein had occurred. The degradation of this protein was prevented by the creation of an N-terminal fusion to the Ubld^{R42P} protein that encoded 56 residues from the B1 immunoglobulin binding domain from protein G (GB1) (*26*) and a 6 residue linker (GB1-Ubld^{R42P}). The addition of the GB1 moiety allowed for the purification of the construct and protected the Ubld from proteolysis as determined by mass spectrometry (MW_{calc} 15451.3, MW_{obs} 15451.4). To determine if any structural changes in the Ubld occurred, or whether an interaction between the Ubld and GB1 domains was evident, a wild-type GB1-Ubld protein was also created and probed by size exclusion chromatography and NMR spectroscopy. Initial size exclusion chromatographic experiments were aimed at examining changes in the apparent protein size of GB1-Ubld compared to GB1-Ubld^{R42P} (Figure 4). These experiments showed that the GB1-Ubld eluted at a smaller volume compared to the GB1 domain alone, consistent with its increased size compared to GB1. In contrast, the elution of the GB1-Ubld^{R42P} was significantly perturbed from the wild-type fusion protein and eluted at a much earlier volume. Despite the near identical molecular weights of GB1-Ubld and GB1-Ubld^{R42P} this difference in elution volume indicates that the GB1-Ubld^{R42P} protein was behaving like a much larger species, consistent with an unfolded or aggregated state.

A more detailed examination of the structural state of the Ubld^{R42P} was completed using $^1H-^{15}N$ HSQC NMR experiments of the GB1, GB1-Ubld, and GB1-Ubld^{R42P} proteins. Due to the small size of the GB1 tag (56 amino acids) and the susceptibility of the Ubld^{R42P} to proteolysis all experiments were completed without cleavage of the GB1 protein. The spectra of the GB1-Ubld and the isolated GB1 domain had well-dispersed peaks with line widths appropriate for proteins in the 8−15 kDa range (Figure 5A). Superposition of these two spectra showed that there was little change in the peak locations for the GB1 moiety when present in the GB1-Ubld fusion protein. Further, all of the resonances from GB1 could be accounted for based on previously published data for this protein (*40*). The data also showed that the subspectrum of the parkin Ubld within in the GB1-Ubld construct was easily identifiable when this spectrum was compared to the $^1H-^{15}N$ HSQC of the Ubld alone. The disperse nature of the Ubld subspectrum indicated that the Ubld was well folded. The similarity of chemical shifts for both the GB1 and Ubld portions of the GB1-Ubld fusion protein, compared to those in the individual domains, provides strong evidence that the GB1 domain and Ubld have little or no association within the GB1-Ubld fusion protein that would alter their structures. This showed that the GB1-Ubld fusion system was a good model for detecting the folded or unfolded state resulting from the R42P mutation in the parkin Ubld. In contrast to the GB1-Ubld protein, the $^1H-^{15}N$ HSQC spectrum of the GB1-Ubld^{R42P} fusion had a mass of peaks located in the central region of the spectrum as well as a group of well-dispersed peaks (Figure 5B). These features of the spectrum indicated that there were two distinct regions within the GB1-Ubld^{R42P} protein, one region that was unfolded and a second that was folded. The location of the well-dispersed peaks was in excellent agreement with those observed in the $^1H-^{15}N$ HSQC spectrum of the isolated GB1 domain and the GB1 portion of the GB1-Ubld fusion protein, indicating that this group of peaks belonged to the GB1 domain that maintained its native fold. The remaining peaks that had little resemblance to the $^1H-^{15}N$ HSQC of the folded wild-type Ubld correspond to the Ubld^{R42P}. The nondisperse nature of these peaks in the $^1H-^{15}N$ HSQC spectrum and their tight clustering between 8.0 and 8.5 ppm in the ^1H dimension indicated that the Ubld^{R42P} was unfolded (Figure 5B). Together with the sensitivity to proteolysis, decreased stability of the similar Ub^{R42P} protein and aberrant behavior in size exclusion experiments, these results show that the R42P mutation in the parkin Ubld causes this domain to unfold.

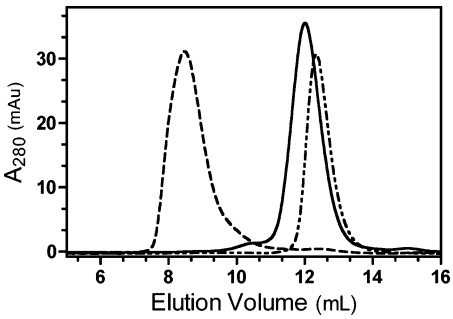

FIGURE 4: Size exclusion chromatography of the GB1 domain, parkin Ubld and parkin Ubld^{R42P}. The elution profiles for the GB1 domain (− ·· −), parkin GB1-Ubld (—), and parkin GB1-Ubld^{R42P} (− − −). All samples were loaded on a Superdex 75 column in 10 mM KH_2PO_4, 1 mM EDTA, 1 mM DTT pH 7 at room temperature and a flow rate of 0.5 mL/min.

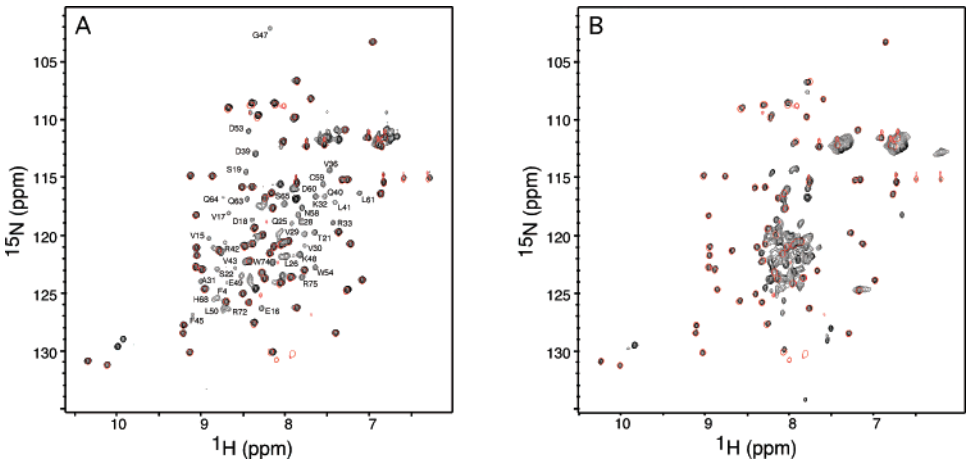

FIGURE 5: $^{1}H-^{15}N$ HSQC spectra of the GB1 fusion proteins. Comparison of the (A) GB1-Ubld with the (B) GB1-Ubld^{R42P}. In both cases the GB1-Ubld or GB1-Ubld^{R42P} protein is plotted in black contours while the isolated GB1 protein is shown in red contours. The spectra were collected at 600 MHz in 10 mM KH_2PO_4, 1 mM EDTA, 1 mM DTT pH 6.8 at 25 °C using protein concentrations of 800 μM. Peaks from the parkin Ubld were labeled according to the published assignment (*14*).

DISCUSSION

The native parkin Ubld and ubiquitin proteins share high sequence similarity (62%) and identity (32%) (*14*) that is also translated into their similar three-dimensional folds (Figure 1). Despite these similarities, there are significant differences between the stabilities of the wild-type proteins. The stability of ubiquitin was about 24.5 kJ/mol at pH 7.0, a value similar to that reported previously (25.2, 28.9 kJ/mol) at pH 5.0 (*41*, *42*). The stability of the parkin Ubld (13.9 kJ/mol) is about 10.6 kJ/mol lower than ubiquitin. This value is similar to at least one other ubiquitin-like protein, SUMO-1 (*43*), indicating that the lower stability of ubiquitin-like proteins may be an inherent property of these proteins compared to ubiquitin. Therefore, mutations when present in the parkin Ubld would be expected to have a larger impact on protein stability *in vivo* on the less stable Ubld than if present in the more stable ubiquitin.

In this work we have examined the structures and stabilities of the disease-causing mutations (R42P, K48A) in the parkin Ubld, the first examples where the stabilities of these proteins were determined using purified proteins. Further, we found that preparing an N-terminal GB1 fusion tag with the Ubld^{R42P} mutant eliminated its degradation and allowed isolation of the fusion protein with an intact Ubld. This protein, as characterized by NMR spectroscopy, showed that the Ubld^{R42P} was unfolded. The two PD causative mutations (R42P and K48A) in the parkin Ubld resulted in drastically different effects in protein stability that was paralleled by the same mutations in ubiquitin. In both cases the K48A mutation had only minor effects on protein stability. This is perhaps not surprising since this residue resides on β-sheet β4 in an exposed position. In parkin, the region of the Ubld that includes Lys48 has been shown to comprise the binding interface with the S5a proteasome subunit (*14*). This interaction surface is also shared by other ubiquitin-like domain proteins including hPLIC-2 (*37*) and hHR23a (*38*). It might be expected that mutation of this residue to alanine, as observed in some ARJP cases, causes a disruption of the parkin interaction with the proteasome. There have, however, been no reports to support this hypothesis. In ubiquitin, the K48A mutation would undoubtedly be detrimental to its function since the Lys48 side chain forms an isopeptide bond in polyubiquitin chain formation, a signal for degradation by the 26S proteasome.

The R42P mutation causes the Ubld in parkin to globally unfold and significantly destabilizes ubiquitin. Within the three-dimensional structures of the parkin Ubld and ubiquitin Arg42 resides near the N-terminus of β-sheet β3. This sheet traverses the central region of each protein possessing several buried hydrophobic residues (V43, I44, F45 in Ubld, L43, I44, F45 in ubiquitin) that stabilize the protein fold. Though similar, the β-sheet β3 in these two proteins is different in length. In the parkin Ubld β3 is only four residues (R42−F45) compared to six residues (Q40−F45) in ubiquitin. In the diseased state, the substitution of a proline at the β-sheet initiating position Arg42 would cause the loss of a hydrogen bond to Val70, in addition to eliminating side chain interactions with Leu50 (β4) and Val70 (β5) across the sheet. This is probably a strong contributor to the global unfolding of the Ubld^{R42P} observed in this work. The unfolding of the Ubld^{R42P} would likely contribute to a more rapid degradation of parkin by the 26S proteasome. This idea is supported by observed decreases in the steady-state levels of the parkin protein containing the R42P mutation (*11*, *21*) and subsequent decreased E3 ligase activity. It has been further shown that the lifetime of the R42P mutant can be increased by the addition of the proteasome inhibitor MG132 (*11*). While the parkin Ubld has been shown to bind the S5a subunit (*14*) of the 19S proteasome lid, the unfolding of the Ubld^{R42P} mutant suggests that this binding is probably not occurring during parkin degradation. However, degradation of parkin could still occur directly by the 20S core of the proteasome as demonstrated for other proteins (*44*, *45*). Consistent with this, a parkin mutant lacking the entire Ubld is degraded more rapidly than the wild-type protein. Further it has been shown that the C-terminus of parkin comprising the IBR-RING domains interacts with subunit α4 of the 20S proteasomal core (*46*). Alternatively, interaction of parkin with the S5a subunit could be promoted through ubiquitination of parkin at a site other than the Ubld.

The parkin Ubld has been shown to interact with, and is required for the polyubiquitination of, substrates p38 (*9*), synphilin (*10*) and α-synuclein (*12*). The R42P mutation causes a decrease in binding of parkin toward p38. Further,

parkin containing the R42P mutation was unable to pull down o-glycosylated α-synuclein (*12*). Our results show the R42P mutant causes the complete unfolding of the Ubld. Thus the decreased interactions with substrates such as p38 and α-synuclein for the R42P mutant are likely a result of Ubld unfolding rather than a modification of the binding site in a structured domain. Taken together, our results show that the R42P and K48A disease state mutations in the parkin Ubld and observed in ARJP lead to dysfunction of the protein by different mechanisms. The R42P mutation destabilizes the domain leading to its complete unfolding and thereby disrupting substrate and/or proteasome interactions. The K48A mutation retains the Ubld but likely leads to a modified interaction with the S5a subunit of the proteasome.

ACKNOWLEDGMENT

The authors would like to thank Kathryn Barber for her excellent technical assistance and Qin Liu for maintenance of the NMR spectrometers in the UWO Biomolecular NMR Facility. We thank Dr. M. Clore for providing us with the GEV1 vector used for the GB1 fusion proteins.

REFERENCES

1. Kitada, T., Asakawa, S., Hattori, N., Matsumine, H., Yamamura, Y., Minoshima, S., Yokochi, M., Mizuno, Y., and Shimizu, N. (1998) Mutations in the Parkin Gene Cause Autosomal Recessive Juvenile Parkinsonism, *Nature 392*, 605−608.
2. Matsumine, H., Saito, M., Shimoda-Matsubayashi, S., Tanaka, H., Ishikawa, A., Nakagawa-Hattori, Y., Yokochi, M., Kobayashi, T., Igarashi, S., Takano, H., Sanpei, K., Koike, R., Mori, H., Kondo, T., Mizutani, Y., Schaffer, A. A., Yamamura, Y., Nakamura, S., Kuzuhara, S., Tsuji, S., and Mizuno, Y. (1997) Localization of a Gene for an Autosomal Recessive Form of Juvenile Parkinsonism to Chromosome 6q25.2-27, *Am. J. Hum. Genet. 60*, 588−596.
3. Shimura, H., Hattori, N., Kubo, S., Mizuno, Y., Asakawa, S., Minoshima, S., Shimizu, N., Iwai, K., Chiba, T., Tanaka, K., and Suzuki, T. (2000) Familial Parkinson Disease Gene Product, Parkin, is a Ubiquitin-Protein Ligase, *Nat. Genet. 25*, 302−305.
4. Hershko, A., and Ciechanover, A. (1998) The Ubiquitin System, *Annu. Rev. Biochem. 67*, 425−479.
5. Glickman, M. H., and Ciechanover, A. (2002) The Ubiquitin-Proteasome Proteolytic Pathway: Destruction for the Sake of Construction, *Physiol. Rev. 82*, 373−428.
6. Pickart, C. M. (1997) Targeting of Substrates to the 26S Proteasome, *FASEB J. 11*, 1055−1066.
7. Zhang, Y., Gao, J., Chung, K. K., Huang, H., Dawson, V. L., and Dawson, T. M. (2000) Parkin Functions as an E2-Dependent Ubiquitin- Protein Ligase and Promotes the Degradation of the Synaptic Vesicle-Associated Protein, CDCrel-1, *Proc. Natl. Acad. Sci. U.S.A. 97*, 13354−13359.
8. Staropoli, J. F., McDermott, C., Martinat, C., Schulman, B., Demireva, E., and Abeliovich, A. (2003) Parkin is a Component of an SCF-Like Ubiquitin Ligase Complex and Protects Postmitotic Neurons from Kainate Excitotoxicity, *Neuron 37*, 735−749.
9. Corti, O., Hampe, C., Koutnikova, H., Darios, F., Jacquier, S., Prigent, A., Robinson, J. C., Pradier, L., Ruberg, M., Mirande, M., Hirsch, E., Rooney, T., Fournier, A., and Brice, A. (2003) The p38 Subunit of the Aminoacyl-tRNA Synthetase Complex is a Parkin Substrate: Linking Protein Biosynthesis and Neurodegeneration, *Hum. Mol. Genet. 12*, 1427−1437.
10. Chung, K. K., Zhang, Y., Lim, K. L., Tanaka, Y., Huang, H., Gao, J., Ross, C. A., Dawson, V. L., and Dawson, T. M. (2001) Parkin Ubiquitinates the Alpha-Synuclein-Interacting Protein, Synphilin-1: Implications for Lewy-Body Formation in Parkinson Disease, *Nat. Med. 7*, 1144−1150.
11. Henn, I. H., Gostner, J. M., Lackner, P., Tatzelt, J., and Winklhofer, K. F. (2005) Pathogenic Mutations Inactivate Parkin by Distinct Mechanisms, *J. Neurochem. 92*, 114−122.
12. Shimura, H., Schlossmacher, M. G., Hattori, N., Frosch, M. P., Trockenbacher, A., Schneider, R., Mizuno, Y., Kosik, K. S., and Selkoe, D. J. (2001) Ubiquitination of a New Form of Alpha-Synuclein by Parkin from Human Brain: Implications for Parkinson's Disease, *Science 293*, 263−269.
13. Sato, S., Chiba, T., Sakata, E., Kato, K., Mizuno, Y., Hattori, N., and Tanaka, K. (2006) 14−3−3eta is a Novel Regulator of Parkin Ubiquitin Ligase, *EMBO J. 25*, 211−221.
14. Sakata, E., Yamaguchi, Y., Kurimoto, E., Kikuchi, J., Yokoyama, S., Yamada, S., Kawahara, H., Yokosawa, H., Hattori, N., Mizuno, Y., Tanaka, K., and Kato, K. (2003) Parkin Binds the Rpn10 Subunit of 26S Proteasomes through its Ubiquitin-Like Domain, *EMBO Rep. 4*, 301−306.
15. Fallon, L., Belanger, C. M., Corera, A. T., Kontogiannea, M., Regan-Klapisz, E., Moreau, F., Voortman, J., Haber, M., Rouleau, G., Thorarinsdottir, T., Brice, A., van Bergen En Henegouwen, P. M., and Fon, E. A. (2006) A Regulated Interaction with the UIM Protein Eps15 Implicates Parkin in EGF Receptor Trafficking and PI(3)K-Akt Signalling, *Nat. Cell Biol. 8*, 834−842.
16. Hartmann-Petersen, R., and Gordon, C. (2004) Integral UBL Domain Proteins: A Family of Proteasome Interacting Proteins, *Semin. Cell Dev. Biol. 15*, 247−259.
17. Jentsch, S., and Pyrowolakis, G. (2000) Ubiquitin and its Kin: How Close are the Family Ties?, *Trends Cell Biol. 10*, 335−342.
18. Biggins, S., Ivanovska, I., and Rose, M. D. (1996) Yeast Ubiquitin-Like Genes are Involved in Duplication of the Microtubule Organizing Center, *J. Cell Biol. 133*, 1331−1346.
19. Takayama, S., Sato, T., Krajewski, S., Kochel, K., Irie, S., Millan, J. A., and Reed, J. C. (1995) Cloning and Functional Analysis of BAG-1: A Novel Bcl-2-Binding Protein with Anti-Cell Death Activity, *Cell 80*, 279−284.
20. Yamanaka, K., Ishikawa, H., Megumi, Y., Tokunaga, F., Kanie, M., Rouault, T. A., Morishima, I., Minato, N., Ishimori, K., and Iwai, K. (2003) Identification of the Ubiquitin-Protein Ligase that Recognizes Oxidized IRP2, *Nat. Cell Biol. 5*, 336−340.
21. Hampe, C., Ardila-Osorio, H., Fournier, M., Brice, A., and Corti, O. (2006) Biochemical Analysis of Parkinson's Disease-Causing Variants of Parkin, an E3 Ubiquitin-Protein Ligase with Monoubiquitylation Capacity, *Hum. Mol. Genet. 15*, 2059−2075.
22. Wang, C., Tan, J. M., Ho, M. W., Zaiden, N., Wong, S. H., Chew, C. L., Eng, P. W., Lim, T. M., Dawson, T. M., and Lim, K. L. (2005) Alterations in the Solubility and Intracellular Localization of Parkin by several Familial Parkinson's Disease-Linked Point Mutations, *J. Neurochem. 93*, 422−431.
23. Beasley, S. A., Hristova, V. A., and Shaw, G. S. (2007) Structure of the Parkin in-between-Ring Domain Provides Insights for E3-Ligase Dysfunction in Autosomal Recessive Parkinson's Disease, *Proc. Natl. Acad. Sci. U.S.A. 104*, 3095−3100.
24. Terreni, L., Calabrese, E., Calella, A. M., Forloni, G., and Mariani, C. (2001) New Mutation (R42P) of the Parkin Gene in the Ubiquitinlike Domain Associated with Parkinsonism, *Neurology 56*, 463−466.
25. Dev, K. K., van der Putten, H., Sommer, B., and Rovelli, G. (2003) Part I: Parkin-Associated Proteins and Parkinson's Disease, *Neuropharmacology 45*, 1−13.
26. Huth, J. R., Bewley, C. A., Jackson, B. M., Hinnebusch, A. G., Clore, G. M., and Gronenborn, A. M. (1997) Design of an Expression System for Detecting Folded Protein Domains and Mapping Macromolecular Interactions by NMR, *Protein Sci. 6*, 2359−2364.
27. Hodgins, R., Gwozd, C., Arnason, T., Cummings, M., and Ellison, M. J. (1996) The Tail of a Ubiquitin-Conjugating Enzyme Redirects Multi-Ubiquitin Chain Synthesis from the Lysine 48-Linked Configuration to a Novel Nonlysine-Linked Form, *J. Biol. Chem. 271*, 28766−28771.
28. Nozaki, Y. (1972) The Preparation of Guanidine Hydrochloride, *Methods Enzymol. 26* (Part C), 43−50.
29. Stoscheck, C. M. (1990) Quantitation of Protein, *Methods Enzymol. 182*, 50−68.
30. Pace, C. N. (1986) Determination and Analysis of Urea and Guanidine Hydrochloride Denaturation Curves, *Methods Enzymol. 131*, 266−280.
31. Santoro, M. M., and Bolen, D. W. (1988) Unfolding Free Energy Changes Determined by the Linear Extrapolation Method. 1. Unfolding of Phenylmethanesulfonyl Alpha-Chymotrypsin using Different Denaturants, *Biochemistry 27*, 8063−8068.
32. Clarke, J., and Fersht, A. R. (1993) Engineered Disulfide Bonds as Probes of the Folding Pathway of Barnase: Increasing the Stability of Proteins Against the Rate of Denaturation, *Biochemistry 32*, 4322−4329.

33. Kellis, J. T., Jr, Nyberg, K., and Fersht, A. R. (1989) Energetics of Complementary Side-Chain Packing in a Protein Hydrophobic Core, *Biochemistry 28*, 4914−4922.
34. Kay, L., Keifer, P., and Saarinen, T. (1992) Pure Absorption Gradient Enhanced Heteronuclear Single Quantum Correlation Spectroscopy with Improved Sensitivity, *J. Am. Chem. Soc. 114*, 10663−10665.
35. Delaglio, F., Grzesiek, S., Vuister, G. W., Zhu, G., Pfeifer, J., and Bax, A. (1995) NMRPipe: A Multidimensional Spectral Processing System Based on UNIX Pipes, *J. Biomol. NMR 6*, 277−293.
36. Johnson, B. A. (2004) Using NMRView to Visualize and Analyze the NMR Spectra of Macromolecules, *Methods Mol. Biol. 278*, 313−352.
37. Walters, K. J., Kleijnen, M. F., Goh, A. M., Wagner, G., and Howley, P. M. (2002) Structural Studies of the Interaction between Ubiquitin Family Proteins and Proteasome Subunit S5a, *Biochemistry 41*, 1767−1777.
38. Mueller, T. D., and Feigon, J. (2003) Structural Determinants for the Binding of Ubiquitin-Like Domains to the Proteasome, *EMBO J. 22*, 4634−4645.
39. Krantz, B. A., and Sosnick, T. R. (2000) Distinguishing between Two-State and Three-State Models for Ubiquitin Folding, *Biochemistry 39*, 11696−11701.
40. Gronenborn, A. M., Filpula, D. R., Essig, N. Z., Achari, A., Whitlow, M., Wingfield, P. T., and Clore, G. M. (1991) A Novel, Highly Stable Fold of the Immunoglobulin Binding Domain of Streptococcal Protein G, *Science 253*, 657−661.
41. Loladze, V. V., Ibarra-Molero, B., Sanchez-Ruiz, J. M., and Makhatadze, G. I. (1999) Engineering a Thermostable Protein Via Optimization of Charge-Charge Interactions on the Protein Surface, *Biochemistry 38*, 16419−16423.
42. Crespo, M. D., Platt, G. W., Bofill, R., and Searle, M. S. (2004) Context-Dependent Effects of Proline Residues on the Stability and Folding Pathway of Ubiquitin, *Eur. J. Biochem. 271*, 4474−4484.
43. Kumar, A., Srivastava, S., Kumar Mishra, R., Mittal, R., and Hosur, R. V. (2006) Residue-Level NMR View of the Urea-Driven Equilibrium Folding Transition of SUMO-1 (1−97): Native Preferences do Not Increase Monotonously, *J. Mol. Biol. 361*, 180−194.
44. David, D. C., Layfield, R., Serpell, L., Narain, Y., Goedert, M., and Spillantini, M. G. (2002) Proteasomal Degradation of Tau Protein, *J. Neurochem. 83*, 176−185.
45. Tofaris, G. K., Layfield, R., and Spillantini, M. G. (2001) Alpha-Synuclein Metabolism and Aggregation is Linked to Ubiquitin-Independent Degradation by the Proteasome, *FEBS Lett. 509*, 22−26.
46. Dachsel, J. C., Lucking, C. B., Deeg, S., Schultz, E., Lalowski, M., Casademunt, E., Corti, O., Hampe, C., Patenge, N., Vaupel, K., Yamamoto, A., Dichgans, M., Brice, A., Wanker, E. E., Kahle, P. J., and Gasser, T. (2005) Parkin Interacts with the Proteasome Subunit alpha4, *FEBS Lett. 579*, 3913−3919.
47. DeLano, W. L. (2002) *The PyMOL Molecular Graphics System*, Palo Alto, CA.
48. Vijay-Kumar, S., Bugg, C. E., and Cook, W. J. (1987) Structure of Ubiquitin Refined at 1.8 Å Resolution, *J. Mol. Biol. 194*, 531−544.

BI7016969